Auto-gyro Descent System for Earth's Atmosphere

Abhay Nudurupati (nabhaykaushik@gmail.com)
University of Petroleum and Energy Studies

Article

Keywords: atmospheric descent mechanism, aerodynamics

Posted Date: September 20th, 2021

DOI: https://doi.org/10.21203/rs.3.rs-871627/v1

Auto-gyro Descent System for Earth's Atmosphere

Abhay Kaushik Nudurupati[1, a)]

[1] University of Petroleum and Energy Studies, Dehradun, India, 248007.

[a)] Corresponding author: nabhaykaushik@gmail.com

Abstract. An atmospheric descent mechanism that utilizes no power would be an efficient way to perform a safe landing procedure for small sized payloads and selected large payloads. This research paper presents the safe landing concept of an auto gyro descent system in the atmosphere of Earth, from a height of less than 1 Kilometre taken from the surface of executing point, using a specialized lift producing blade even at very low free stream velocity. These blades are designed to be highly cambered with suitable parameters as described further in the paper. Most of the parts are designed using CAD software and are 3D printed after a thorough simulation and analysis tests done using COMSOL Multi-physics and Xflr 5 for respective solutions. The model also includes the aerodynamics of the entire structure along with a base casing of specified structural design for further inclusion of electronic components for suitable scientific experiments. This provides a future base line for any kind of atmospheric studies or tests at a reasonable price and can be reused.

Introduction

With vast development of technology far beyond limits of the ground, multiple inventions and innovations awaiting to put on the study with practical research applications as a challenge. Equipment's with physical interactions to surroundings have provided reliable data contributing to the advanced studies of the respective results with safe handling and retrieving of the payload successfully. Numerous active and passive descent mechanisms, few with conventionality satisfy the need and reason to do so involved with any kind of initiation protocols for the same. Example of a study on "Dynamics of a Small Unmanned Aircraft Parachute System" by Panta A, Watkins S and Clothier R [1] involved initiation command prompting the action of passive descent system. Similar active systems undoubtedly have power utilization procedures to involve larger mass and volume to the system to project comparatively a larger factor of limitations in applications. Most atmospheric research experiments involving interaction of samples collected or live data procured for definite altitudes with surface of Earth as reference, following study involving auto-gyro descent system is a passive mechanism, fully autonomous, capable to provide an unpowered safe landing to payloads involving direct environmental contact. The following innovation is the result of observation raised from nature's Maple Seed structure and mechanisms. With curvature similar to airfoil, the lift generated proves sufficient for a float to decrease vertical velocity of falling maple seed as mentioned by Desenfans Philip in "Aerodynamics of Maple Seed" [3]. Similar study presents mechanism with single but much larger maple seed structured blade giving forth the complete analysis with pros and cons of different configuration designs to allow the system compactible into simple CanSat with reference to the study by Chodkaveekityada Peeramed in "CanSat Design and their Applications" [2] or a CubeSat to ensure flexible, easy and cost effective launch. Hence, to start with detailed study of maple seed, the following section involves selection, analysis and fabrication of similar descent mechanism with few changes to further provide advantage to the system.

References

[1] Panta A; Watkins S; Clothier R (2018) Dynamics of a Small Unmanned Aircraft Parachute System. J Aerosp Tecnol Manag, 10: e1218. doi: 10.5028/jatm.v10.752.

[2] Chodkaveekityada, Peeramed. (2018). CanSat design and their applications. 10.2514/6.2018-2407.

[3] Desenfans, Philip: Aerodynamics of the Maple Seed. Project. Hamburg : Aircraft Design and Systems Group (AERO), Department of Automotive and Aeronautical Engineering, Hamburg University of Applied Sciences, 2019.

Study of Auto-Rotating Maple Seed

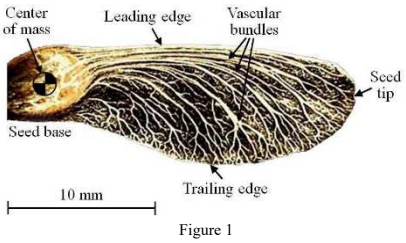

Figure 1

The seeds that are produced by Maple trees have a lot to start with the actual concept of the auto-gyro descent system. These seeds have a peculiar nature to produce lift by themselves primarily due to their structural configuration [4]. The Maple seed is made by nature in a way that places its major mass towards one side that can be taken as its radial centre or the seed root as the torque tends to be zero as the point is approached, same study pointed in by Myong Hwan

[5].The rest of the part is as the configuration of an airfoil shape that produces lift. But, this lift along its length is not equal. Instead, gradually increases as it reaches the tip of the seed. Having such a design forces it to get affected by the torque produced due to the unequal lift along its length and the placing of more mass at its root part. As we know the equation for the lift being, Lift = $C_l(\frac{1}{2})(\rho v^2 s)$ where C_l is the coefficient of lift depending on the airfoil structure, ρ is the density of the fluid medium, v is the velocity of the free stream or the horizontal velocity of the body with respect to free stream and s is the surface area exposed to pressure variation. Taking into consideration the surface area exposed, the tip portion having sufficient surface area to produce a comparatively moderate amount of lift holds the flip action of the seed and the section just before the tip provides the maximum lift when compared to any other part due to its large surface area and optimum linear velocity [5][6][7]. This lift decreases as it reaches the root of maple seed. The same phenomenon is verified and illustrated by a simulation in the figure below.

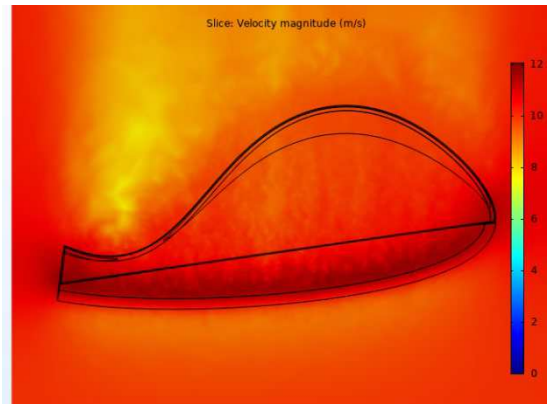

Figure 2
Top Surface Velocity Graph of Maple Seed

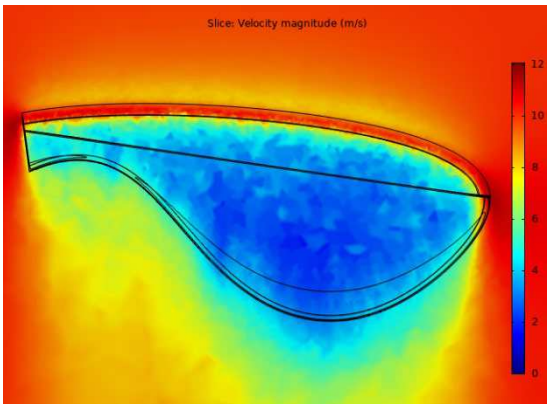

Figure 3
Bottom Surface Graph of Maple Seed

The above velocity magnitude simulations are considered for a random design of a maple seed depicting an unscaled phenomenon of lift distribution. As described by the legend in the figure, the dark blue depicts least velocity tending to zero and the dark red depicts highest velocity possible considering 12 m/sec for this instance. From the Bernoulli's theorem, it can be clearly stated that the velocity at a volume is inversely proportional to the pressure at the same volume. Hence, considering the same from figure 2 and figure 3, the top surface of the seed has a high velocity fluid flow creating a region of low pressure and the bottom surface having a comparitively low velocity has a comparitive high pressure region than the top, creating a notable pressure gradient between the surfaces. This pressure gradient creates an upward force (from the region of high pressure to low pressure) knowm as lift. Understanding the variation of lift can be easy by estimating the amount of pressure difference per unit area of the seed. As seen in figure 3, a good amount of high pressure region lies in the section of larger area as mentioned earlier in the paper. Hence, this variation of lift along its length and concentration of mass at the root of the seed produces a torque with its root as radial center to initiate and continue the rotation movement of the seed to provide linear velocity (free stream velocity) for the specific sections of the blade, this also gradually increases the lift efficiency due to increased angular velocity along time since lift is directly proportional to the square of velocity experienced along the free stream [8][9].

Airfoil Design of Maple Seed Auto-Gyro Blade

Lift is a force that is generated due to the pressure gradient on either sides of a body, usually caused due to changing velocities according to the Bernoulli's theorem. The airfoil shape of the Maple seed is the one that is majorly responsible for the production of lift across its length. Similar to the actual Maple seed considered with random but almost similar airfoil structures, the descent mechanism requires the best airfoil design that can handle a weight of around 100 to 300 grams for a safe landing to be achieved. Having a need to produce a good amount of lift having a decent velocity would be a crucial parameter to be considered as the net lift would be of negative magnitude. This can be satisfied by using airfoils with a high negative camber. Since the mechanism has no external force like motors to drive the rotation of the blade, even a minimum drag produces a huge difference. Having blades of larger thickness would obviously lead to increased interference drag that reduces the angular velocity of the rotor and finally producing less amount of lift force to

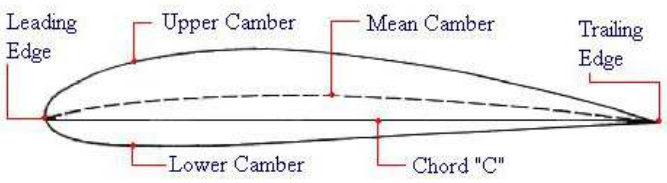

Figure 4

increase the descent velocity which is not actually needed. Hence, a suitable thickness of the blade is to be chosen that can withstand fluid stresses even after being considerably thin. The other important parameter, the drag of the blade has to be minimum as well that can in a way be defined using the position of the maximum camber of the airfoil. Placing the maximum camber towards the leading edge would require more force to enter the fluid section and the one towards the trailing edge wouldn't have the lift required due to the increased flow separation that causes increased drag. Hence, preferring the maximum camber to be placed from 3 to 5 units of the airfoil considering the value to be in tens of chord would be optimum. Since the NACA 950(1-6) theoretically satisfies the analysis, few Good airfoils that can be considered are NACA 6302, Eppler 379, NACA 9501, NACA 9502, NACA 9503, NACA 9504, NACA 9505, and NACA 9506 according to the above theoretical analysis. The diagrams of the same are shown below [10][11].

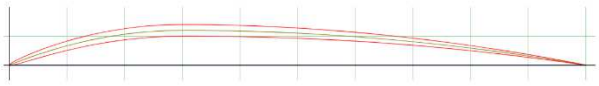

Figure 5 NACA 6302 Airfoil

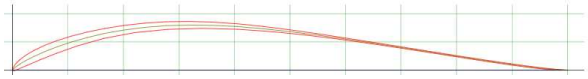

Figure 6 Eppler 379 Airfoil

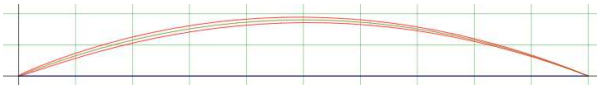

Figure 7 NACA 9501 Airfoil

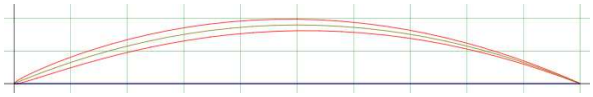

Figure 8 NACA 9502 Airfoil

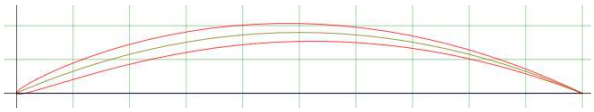

Figure 9 NACA 9503 Airfoil

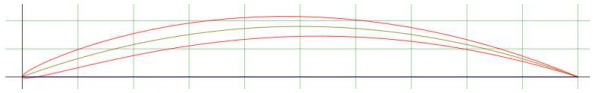

Figure 10 NACA 9504 Airfoil

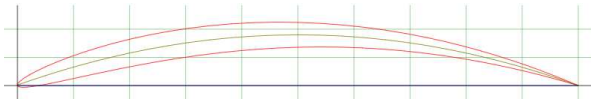

Figure 11 NACA 9505 Airfoil

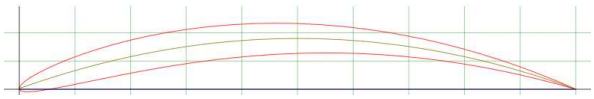

Figure 12 NACA 9506 Airfoil

As in the diagrams, it is clear that all of these airfoils can be a better choice for choosing the rotor blades. But, there will be few disadvantages in their comparison that have to be further described using few simulation tests done on Xflr 5 for choosing the best of these. The Eppler 379 airfoil can be eliminated from the list as it has a trailing edge that is relatively very thin compared to the others mentioned. This increases the probability of damage or complete breakage of the blade during the flight due to pressure gradient between the upper and lower surfaces. Figure 13 and figure 14 show various plots between different variables that describe the results of the airfoils in detail with their specific colours respectively. The C_l vs C_d graph clearly shows the advantage of NACA 9501 over the other airfoils considering the minimum drag coefficient. From the Alpha vs C_l graph that denotes the plot between the angle of attack and the coefficient of lift, it is clear that NACA 9501 has a better C_l than the others at almost the same angles considered. But, NACA 9501 would be eliminated due to its thin structure that makes the blade more prone to fragility damage. It is also be noted from the same graph that NACA 9502 has the highest value of C_l after NACA 9501 at an angle of around 10.0˚. Hence, the considered value of lift coefficient would be 1.1 at an angle of attack at 10.0˚ also reducing the drag force to provide more efficiency of lift.

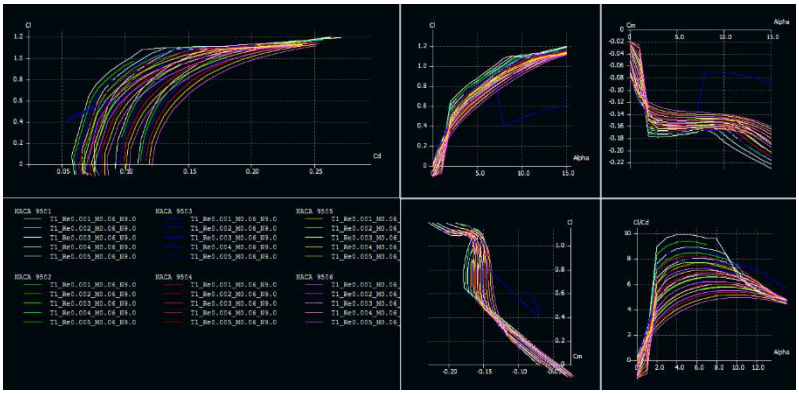

Figure 13 XFLR Analysis of above airfoils [scaled out]

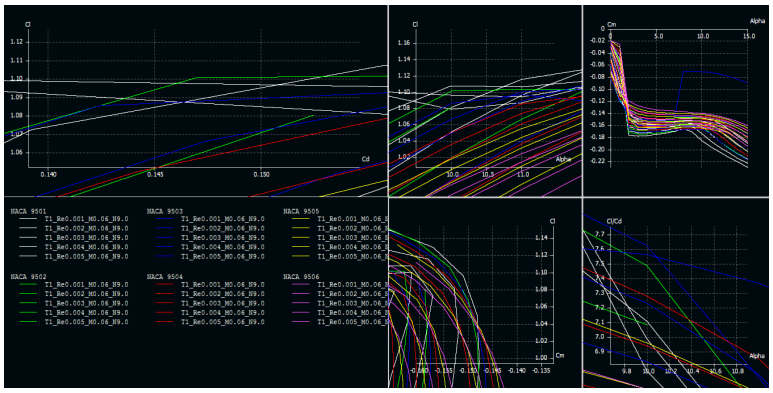

Figure 14 XFLR Analysis of above airfoils [Zoomed in]

Therefore, the airfoil NACA 9502 would be the best to consider for the system's descent control.

For the model size to be easily accessible to be carried by even a CANSAT with a diameter of 12 cm, the blades are preferred to be with a **cord of 10 cm and a span of 26 cm** that allows the maximum possible fit without any frictional or structural limitations and provides the lift force required for the safe descent velocity of a moderately weighing payload.

Design of Maple Seed Blade for Auto-Gyro Blade

A maple seed may have certain variations in their shape depending upon their growth. But, a mechanical system should use the most suitable one for a descent control. This demands analysis of different shapes of maple seed structures that can provide the optimal parameters for the same. Three of the most different ones are shown below.

Figure 15 Blade Design 1

Figure 16 Blade Design 2

Figure 17 Blade Design 3

Different shapes of these provide a large variation on the total system as rotation due to unequal lift at different elements plays a very important role. It is obvious that the lift element graph for each of these blades would be purely unique. The highest positive slope of the graph would decide the shape of the blade that is most optimum for the design. Hence, calculating the same for different elements of each blade considering few standard parameters on a fixed scale as described in the table.

Parameters

Density of Air	1.21 Kg/m^3
Span of Blade	0.08 m
Chord of Blade	0.03 m
Airfoil	NACA 9502
Lift Coefficient	1.10
Angle of Attack	10.0˚
Angular Velocity (Auto-Gyro) [4][5][6]	120 rad/sec

Considering the elemental values for each blade with a length resolution of 1 cm, the graph plotted for three of them on one plane using MATLAB is as follows.

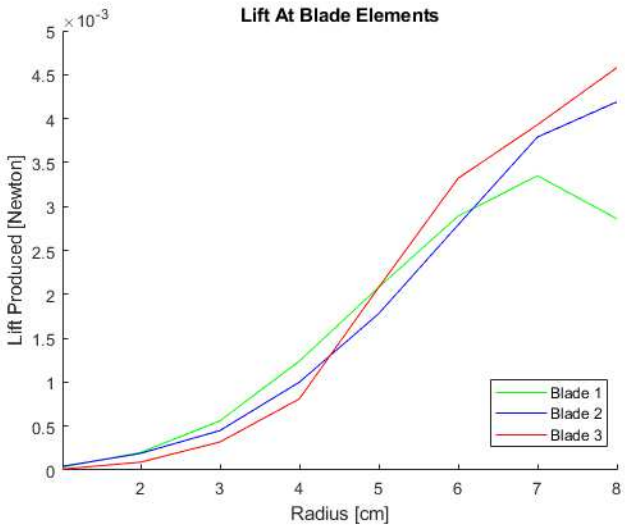

Figure 18 Blade Element Lift Graph of Different Blades.

From the graph plotted for each blade design listed in figure 15, figure 16 and figure 17, using MATLAB taking the values as mentioned in table 1, the graph shows a clear difference in variation of lift force across the length of the blade that has a major effect due to the custom designs. Considering the legend in the graph of figure 18, the blade 3 denoted with the red line has the highest lift and the highest slope denoting a good amount of torque to be produced allowing the rotation of the blade. Hence, the resulting observations demand the consideration of blade 3 to be the most appropriate design. The further mechanism would proceed by considering the same with the NACA 9502 airfoil.

Figure 19 Finalized Blade Design of Blade 3.

Dimensions of Maple Seed Blade

A safe landing velocity would be considered to be around 15 m/sec to 20 m/sec of the whole body. Since the payload is left for free fall, the initial velocity of the payload is considered to be zero and the final velocity as mentioned from 15 m/sec to 20 m/sec. Since having 15 m/sec would be much better than 20 m/sec, a final velocity of 15 m/sec is preferred. The major requirements for descend is shown below in figure 20 with a numerical sketch.

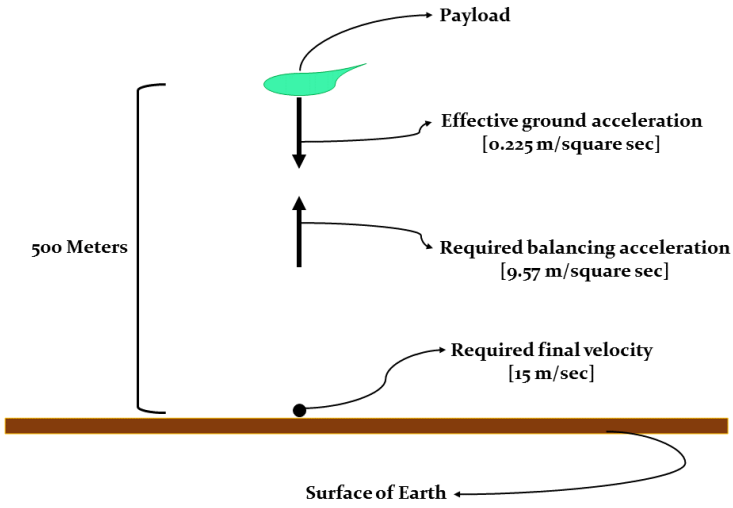

Figure 20 Numerical Sketch of the Descent Situation of Payload.

The mentioned numerical values in figure 20 are derived using the equations of motion as stated further. The maximum altitude of the payload from the surface of Earth is 500 meters [or 0.5 Kilometer], the altitude that can easily be approached by a standard sounding rocket. Since the touch down velocity should be 15 m/sec at the point of touchdown, the final velocity is considered the same and the initial velocity would be zero as mentioned earlier. Calculating the effective descent acceleration of the payload, the equation $V^2 - U^2 = 2aS$ the solution is as follows.

$$V^2 - U^2 = 2aS$$

Where, 'V' is the final velocity; 'U' is the initial velocity; 'a' is the acceleration; 'S' is the altitude from surface of Earth.

$15^2 = 2(a)(500)$ Hence, **the effective acceleration 'a' = 0.225 m/square sec**. …….. (Equation 1)

The acceleration that should be acted on the payload for the required final velocity is calculated as 0.225 m/square sec. For the total lift force to be known for the blade design, equation from the Newton's second law of motion F=ma is solved for the force F. Where the acceleration required to balance the downward acceleration i.e. gravity is 'a_b' is known from the difference of acceleration due to gravity (9.8 m/sec) and the effective acceleration calculated from the equation 1 mentioned above. Hence, the **balancing acceleration 'a_b' is calculated to be 9.57 m/square sec. The mass of the payload is taken to be 417.9 grams [0r 0.4179 Kilograms]**. Therefore, using the equation F = ma.

F = (0.4197) (9.57)

F = 4.0165 Newton's ……. (Equation 2)

From the result in equation 2, it is clear that to maintain the velocity of 15 m/sec at the point of touchdown for safe landing, the lift produced by the designed blade should qualify a value of 4.0165 newton of force. This lift force can be calculated precisely using the blade element theory that calculates the lift produced by each section of the blade using the equation of lift noted as

$$Lift = C_l \frac{1}{2} \rho V^2 S$$

Where;

C_l is the coefficient of lift by the airfoil used

ρ is the density of air

V is the free stream velocity with respect to the blade's position

S is the surface area of the blade exposed to the pressure gradient

From the previous data in the paper, the values of C_l and the dimensions are taken to be 1.1 and 10 cm chord along with 25 cm of span respectively. The value of ρ i.e. the density of air is a constant value of 1.225 kg/m^3 and the angular velocity of an average auto-gyro rotating blade is 12 rad/sec with the same value considered for the further calculation. The blade element analysis of the maple seed blade derived so far is listed below to obtain the induced lift of each element of the blade.

Blade Element Analysis of Maple Seed

1	Region 1	0 to 1	0.000227	1.200	0.000220
2	Region 2	1 to 2	0.000230	2.400	0.000893
3	Region 3	2 to 3	0.000231	3.600	0.002017
4	Region 4	3 to 4	0.000245	4.800	0.003803
5	Region 5	4 to 5	0.000268	6.000	0.006500
6	Region 6	5 to 6	0.000301	7.200	0.010513
7	Region 7	6 to 7	0.000339	8.400	0.016116
8	Region 8	7 to 8	0.000378	9.600	0.023471
9	Region 9	8 to 9	0.000421	10.80	0.033085
10	Region 10	9 to 10	0.000469	12.00	0.045502
11	Region 11	10 to 11	0.000527	13.20	0.061867
12	Region 12	11 to 12	0.000603	14.40	0.084244
13	Region 13	12 to 13	0.000741	15.60	0.121497
14	Region 14	13 to 14	0.000872	16.80	0.165819
15	Region 15	14 to 15	0.000931	18.00	0.203233
16	Region 16	15 to 16	0.000954	19.20	0.236946
17	Region 17	16 to 17	0.000954	20.40	0.267490
18	Region 18	17 to 18	0.000939	21.60	0.295170
19	Region 19	18 to 19	0.000913	22.80	0.319771
20	Region 20	19 to 20	0.000875	24.00	0.339570
21	Region 21	20 to 21	0.000826	25.20	0.353411

22	Region 22	21 to 22	0.000765	26.40	0.359226
23	Region 23	22 to 23	0.000692	27.60	0.355159
24	Region 24	23 to 24	0.000601	28.80	0.335860
25	Region 25	24 to 25	0.000468	30.00	0.283784
26	Region 26	25 to 16	0.000175	31.20	0.114775

Effective Lift	**4.039941906**
Average Lift	**0.155382381**

Table 1 Blade Element Analysis of the Maple Seed Blade Chosen

From table 1, the blade element analysis of the chosen maple seed blade describes the lift induced per every centimetre in the section of blade span. This gives the precise values of average lift and the effective lift of the blade. As seen at the bottom of the table, the effective lift of the blade is calculated to be 4.039941906 Newton of force. Hence, satisfying the demanded lift from equation 2. As described in the previous section of 'Study of Auto-Rotating Maple Seed', the slope of the lift curve across the span of the blade is directly proportional to the rotating nature of the wing due to the influence of torque. The similar graph of the blade considered can be obtained from table 1 and is plotted in figure 21.

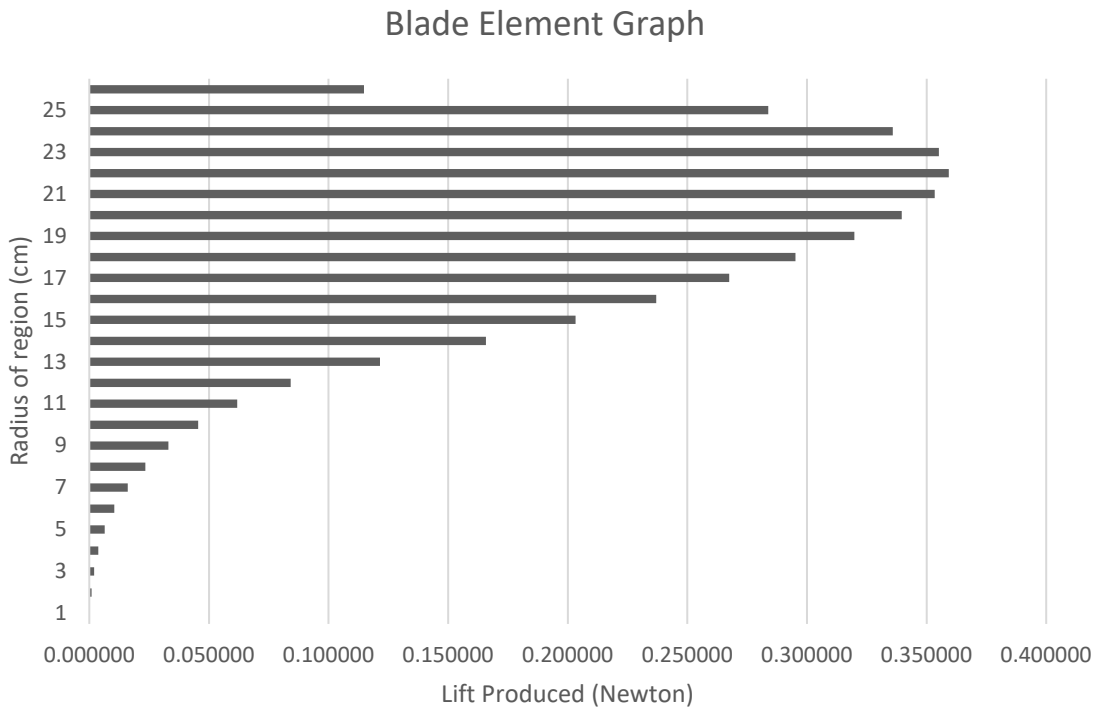

Figure 21 Blade element graph of the chosen maple seed blade.

In the figure 21, the slope between the highest point of lift and the lowest point of lift from the graph is an important parameter that defines and maintains the rotation of blade caused by the free stream air flow. Figure 22 shows the separated regions listed in table 1 and in figure 21, starting from the root of the blade. Each section has a length of 1 cm through the span of the blade i.e. the analysis is done with a resolution of 1 cm span and existing variable chord of the blade at each section as the chord is not constant across the blade due to the maple seed design. The upper border shown in the figure 22 acts as the leading edge of the NACA 9502 airfoil and the bottom border as the

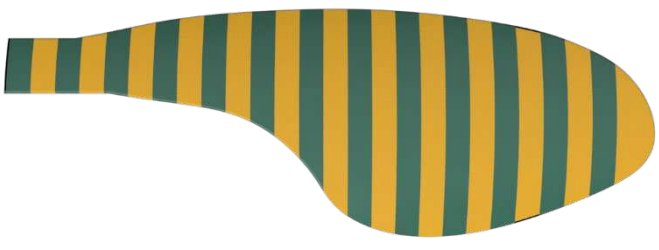

Figure 22 depiction of sections of blade for blade element analysis.

trailing edge. The region 22 of the blade has the highest lift produced per section due to its optimum position to suitable velocity and enough surface area as the angular velocity is converted to linear velocity at every section as it varies with the length or span of the blade. It is calculated using the formula v = (r) (ω) where v is the linear velocity, r is the radius from the root and ω is the angular velocity. Since the free flow velocity of the air is considered parallel to the surface of the blade, it should be converted into linear velocity that is considered in table 1.

Design and Simulation of Final Blade

From all the above discussions, the final blade design is ready after theoretical and numerical analysis. The blade has the specifications of,

Maximum Span: 26 cm (0.26 meters)

Maximum Chord: 10 cm (0.10 meters)

Airfoil design: NACA 9502 with an angle of attack of 10˚ having a lift coefficient of 1.1

Shape: Shape 3 considered from figure 17 or figure 19.

This produces a lift of approximately 4 newton to safely land a mass of around 400 grams (0.4 Kilograms) from a height of 500 meters (0.5 Kilometre). The computer aided design of the final blade is crafted on fusion 360 software and is shown below in the following from figure 23 to figure 25.

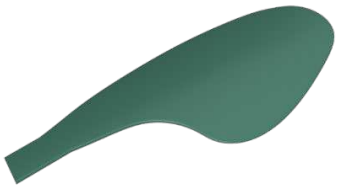

Figure 23 Isometric view of the final blade.

Figure 24 Side view of final blade.

Figure 25 Zoomed isometric view of final blade.

All the theoretical parameters and calculations of the blade satisfy the desired results. The same can be verified by simulations using COMSOL Multi-physics to have a deeper look at the parameters and their effect on the blade elements. The pressure distribution along the surfaces of the blade is shown in the figures. The pressure distribution on the upper surface of the blade when positioned at an angle of attack equal to 10˚ in the free stream is in figure 26. The majority of blue region on its surface represents the low pressure region from -318 to -4 Pascal's of pressure referring form the legend included. A low pressure region created on the upper surface of a blade is a good sign to provide the high lift required (4 newton approx. in this case). This would also depend on the pressure distribution on the bottom surface and the gradient of it with the upper surface. The simulation result of the bottom surface of the same blade is provided in figure 27 following the text. The data in figure 27 details the pressure distribution due to the flow velocity on the lower surface of the final blade considered. This pressure ranges from 19 Pascal to 284 Pascal at the major portion of the lower surface generating a maximum pressure difference of around 500 Pascal on either sides of the blade.

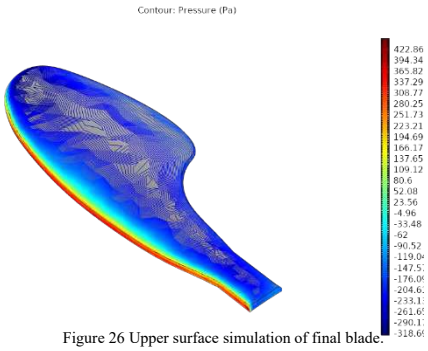

Figure 26 Upper surface simulation of final blade.

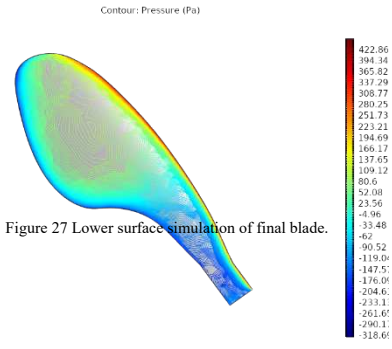

Figure 27 Lower surface simulation of final blade.

The free flow velocity for the simulation is given to a varying average between the maximum velocity of 31.2 m/sec and minimum velocity of 1.2 m/sec as mentioned in table 1 above. The velocity illustration for the same simulated on COMSOL Multi-physics is shown in figure 28. The fluid flow along the surface of the blade viewed from the side of its cross-section, reveals the varying velocity of fluid at different sections as mentioned in the legend of the simulation provided. This simulations if done taking a free flow velocity of 27 m/sec, the highest linear velocity that can be achieved by the blade at the section of maximum lift.

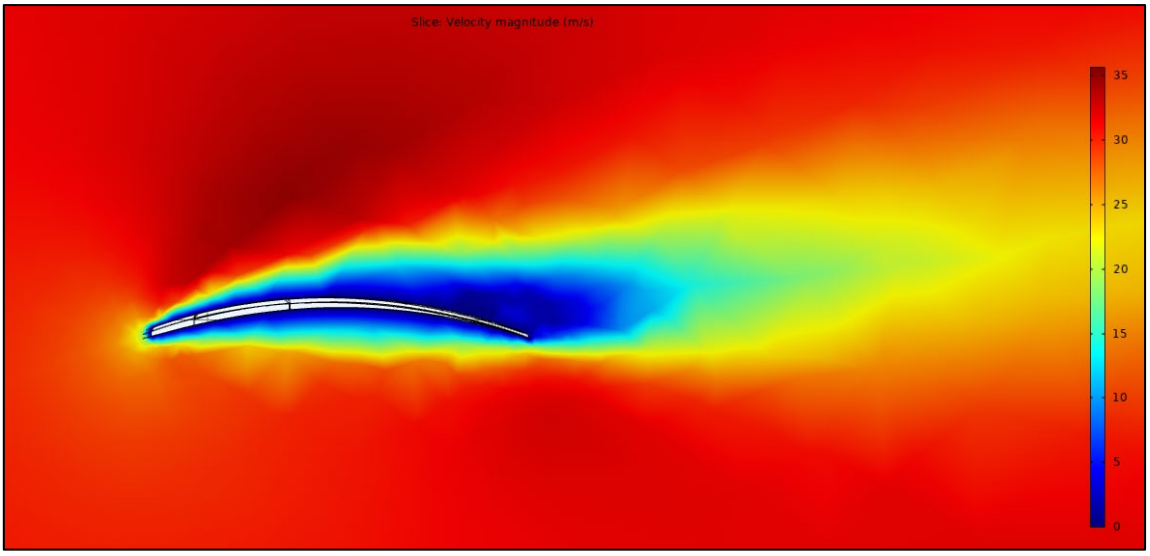

Figure 28 Free Flow Velocity Distribution along the Blade.

At an angle of attack equal to 10˚, the maximum velocity of free flow that is achieved in greater than the initial free flow velocity visible above the top surface of the blade being close to 35 m/sec caused due to the venture effect by the curved airfoil surface. The velocity of flow below the blade is a mixture of normal and low velocity flow varying from 0 to 18 m/sec. According to the Bernoulli's theorem, higher velocity in a volume results in decrease of static pressure at that volume and vice-versa. Relating this to the simulation result in figure 28, the higher velocity above the blade creates a low pressure region than the high pressure at the lower section due to reduced velocity of the free flow. The pressure gradient caused is the result of upward force acting on the blade technically known to be the lift force.

As per the study of maple seed's rotation, the rotational motion of the maple seed primarily depends on the distribution of mass along the span and then on the centre of lift. Having a raised seed tip is necessary for sufficient torque to be produced for the rotation of the complete system. Hence the majority of the mass in the system should be placed at the root of the blade to ensure easy path through the fluid and have it lowered relative to the tip.

Design and Structure of Payload Casing

The principle motive of the descent mechanism being to perform experiments in the atmospheric layers, sensors according to the requirements are a must. Since, any kind of such devices cannot be placed on the surface of the blade with two major reasons involving exposure to atmosphere and interfering aerodynamic flow over the surface of the blade structure, a specially designed casing structure is designed and placed at the root of the blade with reference to the major mass concentration from study of the maple seed aerodynamics and rotation. Also, taking into consideration the factors that can influence the descent velocity in a positive point including the shape, volume, and orientation of the casing, different views of the same are shown in figure 29.

Figure 29 Top View, Side View, and Front View of Casing (From Left).

This payload casing is installed in the at the root of the blade with a reverse airfoil structure, narrowing the airflow at the bottom surface, increasing velocity of free flow to generate a region of low pressure according to the Bernoulli's theorem. The same pressure gradient creating a force acting downward only at the root of the blade. Such an action of the free flow

along the surfaces of the structure creates an angle of elevation from the root to tip of the blade increasing the torque acting for rotation to have an additional amount of negative lift supporting the descent velocity of the entire system. Also, having least surface area of the casing exposed to free flow, this structure produces a least amount of drag that would be considered the major factor when modelling any autogyro systems. A clear view of the complete design is presented in figure 30 following the text.

Providing sufficient space for the devices like tiny microcontrollers, sensors etc. the dimensions of the casing are listed as 6 x 5 x 3.5 l x b x h (in cm) with a total utilisable volume of 24.045 cm^3. The same are listed below in table 2.

Parameter	Value
l x b x h	6 x 5 x 3.5 (cm)
Utilisable Volume	24.045 (cm^3)
Surface Area	65.58 (cm^2)

Table 1 Specifications of Casing.

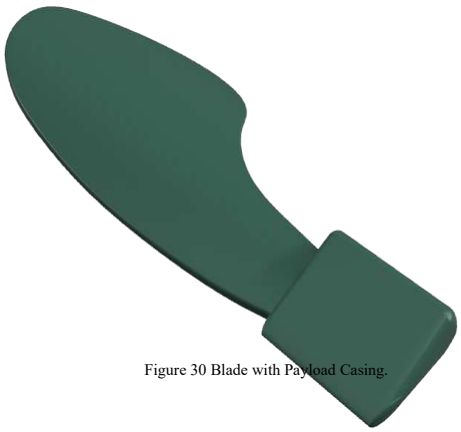

Figure 30 Blade with Payload Casing.

Simulation of Blade with Payload Casing

Analysis of the structural and design part of the payload uses real time simulations, providing a major result of the structure. This simulation is done on COMSOL Multiphysics and verifies the theoretical analysis, making the idea more sustainable. In figure 31 and figure 32 are the flow simulations of the completed blade along with the casing. From figure 31, the pressure distribution on the upper surface of the entire structure is presented with the gradient mentioned in the legend. Following the same, the pressure above varies from -783 Pa to -135 Pa and concentrating on the casing surface, the pressure shows a good increase as discussed earlier about the downward force. The pressure gradient from 263 Pa to -85 Pa is a fairly high pressure region as compared to the bottom surface of the installed casing shown in figure 32, hence

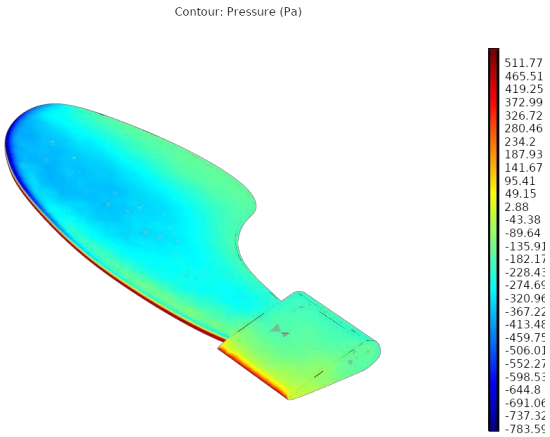

Figure 31 Pressure Distribution on Upper Surface of Final Blade.

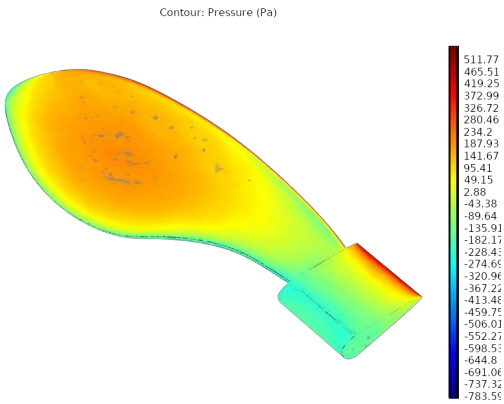

Figure 32 Pressure Distribution on Lower Surface of Final Blade.

satisfying the condition. For the final review, it also clear about the pressure distribution on the surface of the actual blade as well. As comparing with pressure gradient of lower surface, the lower surface as shown in figure 32 has a distribution from -36 Pa to 412 Pa. This gradient between the surfaces would be sufficient for the mentioned mass to be handled as analyses previously by the blade element theory and the C_l of the NACA 9502 airfoil derived from the analysis using Xflr 5 software. Hence, the final simulation of the blade would sufficiently

provide and verify the data that is required.

Results and Conclusion

The above study focused on auto-gyro descent mechanism with concept of maple seed aerodynamics can develop a launch ready passive safe landing system with no initiation protocols or even microcontrollers. The final dimensions were obtained after iterative design optimisation Analysis with simulations and theoritical procedures from the study to provide a maple seed shaped aerodynamic structure with maximum cord and span of 10 cm and 26 cm respectively. The 15 m/sec touchdown velocity of the system is a key factor for safe recovery of the system, requiring no telemetry instruments that occupy volume, mass and complexity on a whole. The final design was successfully simulated to obtain required conditions to match the data obtained theoritically and selected practical procedures. Studies have also been performed to understand present and future research based works in the atmospheres of not only Earth, rather including atmosphere on planets with sufficient density like Mars. Numerous activa and passive mechanisms already in use have shown their ability with similar descent environmental parameters, proving the definite possibility of this type of passive mechanism to reach the abilities.

Acknowledgements

The author wishes to thank University of Petroleum and Energy Studies [UPES] Dehradun, family, friends and colleagues for providing educational resources and support for this project. Gratitude is also expressed to the teams behind the various studies related to the present one for providing reliable public data for research purposes. The author would like to specially thank Mr. Kumar Gourav, University of Petroleum and Energy Studies [UPES] for the invaluable guidance and support provided.

References

[1] Panta A; Watkins S; Clothier R (2018) Dynamics of a Small Unmanned Aircraft Parachute System. J Aerosp Tecnol Manag, 10: e1218. doi: 10.5028/jatm.v10.752.

[2] Chodkaveekityada, Peeramed. (2018). CanSat design and their applications. 10.2514/6.2018-2407.

[3] Desenfans, Philip: Aerodynamics of the Maple Seed. Project. Hamburg : Aircraft Design and Systems Group (AERO), Department of Automotive and Aeronautical Engineering, Hamburg University of Applied Sciences, 2019.

[4] Minami, Shizuka & Azuma, Akira. (2003). Various flying modes of wind-dispersal seeds. Journal of theoretical biology. 225. 1-14. 10.1016/S0022-5193(03)00216-9.

[5] Sohn, Myong. (2016). Aerodynamic Features of Maple Seeds in the Autorotative Flight. Journal of the Korean Society for Aeronautical & Space Sciences. 44. 843-852. 10.5139/JKSAS.2016.44.10.843.

[6] Lugt H J 1983 Autorotation Annu. Rev. Fluid Mech.

[7] Smith, E. (1971). Autorotating wings: An experimental investigation. *Journal of Fluid Mechanics, 50*(3), 513-534. doi:10.1017/S0022112071002738

[8] Skews, B. Autorotation of many-sided bodies in an airstream. *Nature* **352,** 512–513 (1991). https://doi.org/10.1038/352512a0

[9] "Spinning Seeds Inspire Single-Bladed Helicopters", Jacob Aron: https://www.newscientist.com/article/dn20045-spinning-seeds-inspire-single-bladed-helicopters/ [Accessed 17 August 2021]

[10] "NACA 4-Digit Airfoil Equations" Aerospace web: http://www.aerospaceweb.org/question/airfoils/q0100.shtml [Accessed 21 August 2021]

[11] Airfoil Tools, 2017. *Airfoil database search*. [online] Airfoiltools.com.[Accessed 21 August 2021].